Multifunctional hardmask neutral layer
for directed self-assembly (DSA) patterning

Douglas J. Guerrero, Mary Ann Hockey, Yubao Wang, and Eric Calderas
Brewer Science, Inc., 2401 Brewer Drive, Rolla, MO, USA 65401

ABSTRACT

Micro-phase separation for directed self-assembly (DSA) can be executed successfully only when the substrate surface on which the block co-polymer (BCP) is coated has properties that are ideal for attraction to each polymer type. The neutral underlayer (NUL) is an essential and critical component in DSA feasibility. Properties conducive for BCP patterning are primarily dependent on "brush" or "crosslinked" random co-polymer underlayers. Most DSA flows also require a lithography step (reflection control) and pattern transfer schemes at the end of the patterning process. A novel multifunctional hardmask neutral layer (HM NL) was developed to provide reflection control, surface energy matching, and pattern transfer capabilities in a grapho-epitaxy DSA process flow. It was found that the ideal surface energy for the HM NL is in the range of 38-45 dyn/cm. The robustness of the HM NL against exposure to process solvents and developers was identified. Process characteristics of the BCP (thickness, bake time and temperature) on the HM NL were defined. Using the HM NL instead of three distinct layers – bottom anti-reflective coating (BARC) and neutral and hardmask layers – in DSA line-space pitch tripling and contact hole shrinking processes was demonstrated. Finally, the capability of the HM NL to transfer a pattern into a 100-nm spin-on carbon (SOC) layer was shown.

Keywords: DSA, BCP, hardmask neutral layer, pattern transfer, grapho-epitaxy

1. INTRODUCTION

Directed self-assembly (DSA) is currently being explored as a new method for substituting resist in sub–14 nm technologies. In addition to providing resolution beyond the current optical limits, DSA has the potential to reduce or eliminate problems with pattern collapse and line edge roughness (1-3). At least three DSA process flows have been investigated (4). The proposed flows have several things in common. All of them need a pattern transfer scheme into the substrate after the patterns are formed. If a pre-pattern is utilized, some sort of reflection control is also needed during the lithographic step. Finally, all DSA flows require a crosslinked neutral layer ("brush" or "mat") on which the block co-polymer (BCP) can be coated. The neutral layer provides the surface energy required to induce pattern formation.

The goal of this paper is to develop and characterize a new multifunctional layer that could simplify and reduce the number of layers used in current DSA processes. We have developed DSA-enabling hardmask neutral layers (HM NLs) that have all of the required characteristics for DSA process flows (reflection control, neutral layer, pattern transfer) in a single coating application. The reflection control property is needed to control critical dimensions (CD) and reflectivity during a pre-pattern lithography step. Due to the selection of hardmask polymer types, this material has also high absorbance. Measured k-values are as high as other standard bottom anti-reflective coatings (BARCs) utilized in ArF lithography. The neutral underlayer property replaces the need for a separate brush layer. The type of polymer and total inorganic content in the HM NL also provide inherently good etch resistance and pattern transfer capability.

With the requirement to form a guide layer or pre-pattern with a range of photoresists, the NL must also have the ability to maintain the surface properties required for successful DSA imaging upon being subjected to various solvents for either positive-tone or negative-tone development steps. The HM NL developed as a neutral underlayer is capable of being crosslinked sufficiently to provide resistance to a wide range of solvents used for standard development steps at pre-patterning, such as TMAH, n-butyl acetate, or 2-heptanone.

Conventional Process

Litho	PR hardening and BCP coat	PMMA removal	NL, BARC etch

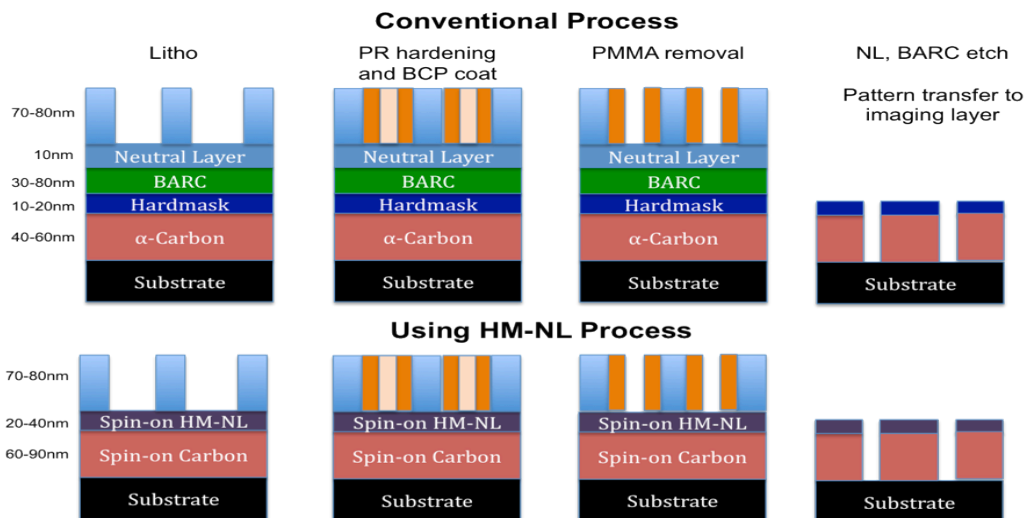Pattern transfer to imaging layer

Using HM-NL Process

Figure 1. Process flow using a hardmask neutral layer (HM NL; Brewer Science) eliminates the "brush" layer, BARC, and hardmask.

Figure 1 above compares a typical process flow (top) using poly (styrene-block-methyl methacrylate) (PS-b-PMMA) BCP and an improved flow (bottom) showing the advantages of using a multifunctional HM NL. The improved process using HM NL steps eliminates the need for a specific BARC, standard "brush" layer, and a separate hardmask deposition step (SiN or other CVD process).

2. EXPERIMENTAL

2.1 Materials and HM NL screening process

Three different types of monomers were formulated using ratio variations in order to understand the effect of both the type and concentration on surface energy information. These monomers were dissolved in PGME/PGMEA solvents at 1.5% solids. Each of the materials was coated onto 110-nm spin-on carbon (SOC) substrates to a thickness of 20-40 nm and baked at 240˚C for 1 minute. Contact angle was measured prior to performing the process steps of PS-b-PMMA coating and annealing.

Commercially available BCPs from Polymer Source Inc. ($L_0 = 25$ nm) were blended with PGMEA in-house in order to achieve 1% solids content. BCP, at a thickness of 25-30-nm, was coated on the HM NL materials. BCP annealing temperatures in the 210º-230ºC range were selected with variations in time of 1-5 minutes throughout the project. Materials were quickly screened for their ability to induce fingerprint patterns either by SEM inspection or using the Digital Instruments (Veeco) Dimension 3100 Nanoscope IIIA atomic force microscope (AFM).

2.2 Surface energy measurement

Surface energy measurements were obtained using contact angle measurements of H_2O and methylene iodide (MI). The shape of static liquid droplets dispensed onto the surface of the HM NL was measured using a goniometer. The slope of the tangent at the liquid-solid-vapor (LSV) interface and liquid drop shape were used to determine the contact angle and surface energy values. Three measurements per substrate were averaged for each contact angle test.

In addition to measurements taken on coated HM NL surfaces, we studied solvent compatibility and how each material behaves after being subjected to varying solvents. The HM NL was coated at a thickness of 30 nm and baked at the same temperature used for BCP annealing (230º-240ºC), and then each solvent was dispensed for 10 seconds.

The solvents then remained on the surface for 30 seconds (total dwell time). A spin-dry removal step followed by a bake of 150ºC for 30 seconds was performed on a standard Brewer Science® Cee® 100CB spin coater/bake plate tool. Contact angle measurements for surface energy calculations were repeated after post-solvent processing. We used both negative-tone (2-heptanone, n-butyl acetate) and positive-tone (TMAH) developers.

2.3 Lithography process

We utilized a grapho-epitaxy process flow with negative-tone photoresist as previously described (4) to evaluate the HM NL performance on its ability to form lines/spaces and contact hole shrink. The HM NL was coated on top of a 100-nm SOC layer. All SOC, HM NL, and BCP coatings and the resist hard bake were done on a TEL CLEAN TRACK ACT12 under N_2 atmosphere. All layers, with the exception of the resist, were baked at 240°C for 1 minute; for the BCP, for up to 5 minutes. The resist was hard baked at 200°C for 5 minutes.

Pre-patterns for lines/spaces were carried out on ASML XT 1250D scanner using negative-tone photoresist (from FUJIFILM Electronic Materials), 0.85 NA using dipole illumination (σ_o = 0.93, σ_I = 0.69). For the contact hole shrink process, pre-patterns were prepared in a Sokudo DUO track interfaced to an ASML NXT 1950i scanner, NA 1.30 using Quasar 30 illumination (σ_o = 0.80, σ_I = 0.65) and SG-N003i resist (TOK).

2.4 Pattern transfer process

An Oxford PlasmaLab80+ etch tool was utilized for etch pattern transfer work. Bulk etch rates were calculated on blanket substrates to determine the etch rate followed by DOE work for power, pressure, and flow settings. Low power (~200 watts), low pressure (10-15 mTorr) gas flows combining Ar: CF4 (1:3 range) were used to successfully etch through the HM NL.

Following the HM etch process, the 110-nm SOC material etch was accomplished using low power (~200 Watts), medium pressure (30 mTorr) and N_2: Ar:O2 gas ratios of 1:1:3 ranges.

3. RESULTS AND DISCUSSION

3.1 Surface energy effects

Formulations with values of surface energy measured from low to high show a trend in imaging for "fingerprints" (Figure 2). When total surface energy (in dyne/cm) was in a specific range, good DSA imaging resulted. With increasingly high measurements in surface energy, the hardmask materials are less likely to provide good imaging, with the resulting "fingerprint" pattern visually intermittent with "dewetting" type patterns or isolated islands visible (Figure 3). Total surface energy values in the ranges of 38-45 dyn/cm after exposure and development of the pre-pattern layer have been targeted for the most robust materials and successful DSA imaging of lines and spaces.
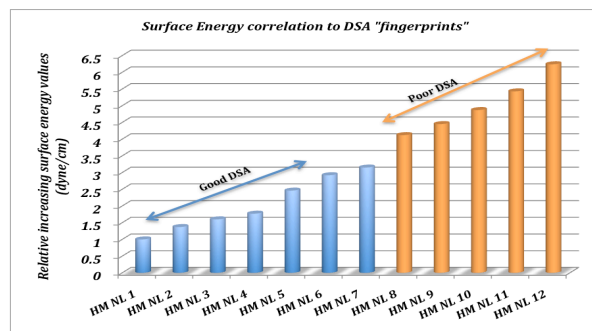

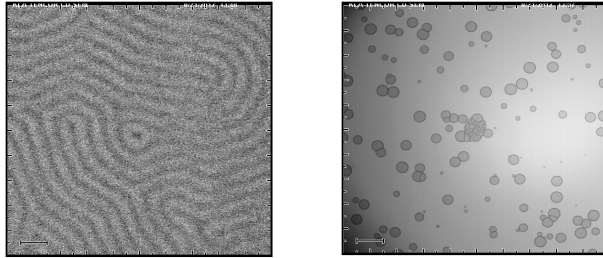Figure 2. Relative values of surface energy as a function of HM NL type.

Figure 3. Effect of HM NL surface energy on pattern formation.
BCP coated on HM NL with low (left) and high (right) surface energy.

An important value to identify is the change in surface energy that occurs during a pre-pattern litho process. If the HM NL has an ideal surface energy for BCP pattern formation at the beginning but changes during the process, the end result will not yield the desired alignment. We studied the changes of surface energy on the HM NL as it is exposed to various NTD and PTD developers and rinses. The results are summarized in Table 1. There is minimal change (1-1.5%) to the surface energy or contact angles with solvents used for development of negative-tone photoresist. Positive-tone expose and development results are also summarized here. We observed a change in the range of 5-7% in total surface energy in the test performed by coating 193-nm photoresist (JSR 1682J) onto the neutral layer, blanket exposing the photoresist (17 mJ/cm^2), and developing for 60 seconds using 2.38% TMAH solution.

Process	H$_2$O Contact Angle (°)	Polar Energy (dyn/cm)	Total Energy (dyn/cm)
After HM NL coat	72.0	9.0	41.0
After n-butyl acetate rinse	71.6	8.7	41.4
After 2-heptanone rinse	71.3	8.8	41.6
After resist coat + exposure + TMAH develop	68.4	9.8	44.2

Table 1. HM NL characteristics after various litho steps and solvent processing.

The observed change using TMAH developer is significant as it results in a diminished ability of the HM NL to induce BCP patterns. To understand this effect, we printed open squares using a PTD resist and process on a wafer coated with the HM NL. The resist was removed with pre-wet solvent, and the wafer was then coated with BCP and baked using the standard process. The open square was the area exposed and developed, while the unexposed areas were in contact with only resist and solvent. The results show a clear delineation on the areas where the developer was in contact with the HM NL. These areas no longer induced BCP alignment, while the areas that were covered with resist still show pattern formation (Figure 4). The ability of the HM NL to change surface energy values is not necessarily a negative property of these materials but instead could be utilized for chemo-epitaxy flows in the future.
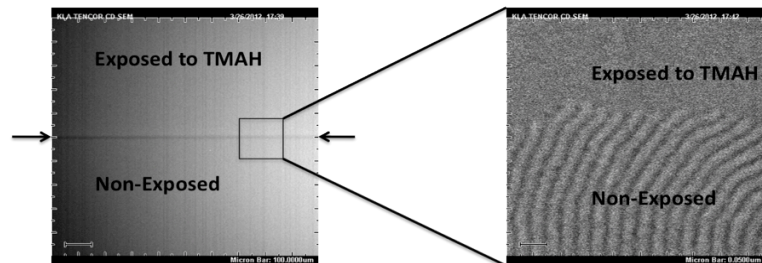

Figure 4. CD SEM photos showing the effect of TMAH rinse on HM NL's ability to induce patterns post-processing.

3.2 BCP thickness, bake temperature, and time effects on HM NL

A BCP (L_0 = 25 nm) coated on a 40-nm HM NL was studied to understand the effects of thickness change, anneal temperature, and anneal time. To obtain a range of BCP thicknesses, we varied spin speeds from 1000–2000 rpm, as shown in Figure 5. Based on the results of this test, good fingerprints were achieved using 17- to 26-nm BCP thicknesses. Hardmask materials developed for neutral layers were screened for minimum and maximum thicknesses that are capable of achieving good imaging.
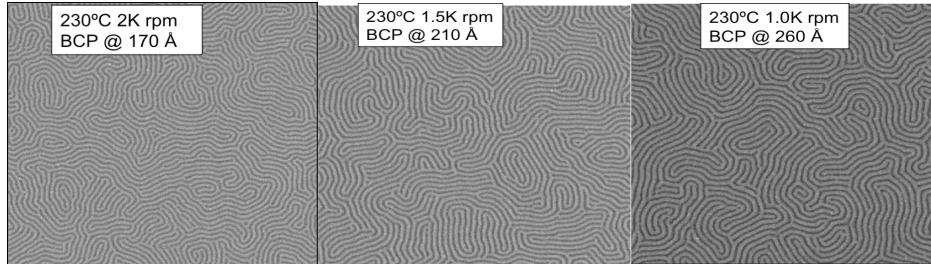
Figure 5. Good fingerprints on HM NL using a range of BCP thicknesses (17-26 nm).

The impact of temperature for the BCP annealing step is shown in Figure 6. We were able to anneal the BCP as low as 210ºC for 5 minutes while achieving good BCP patterning.
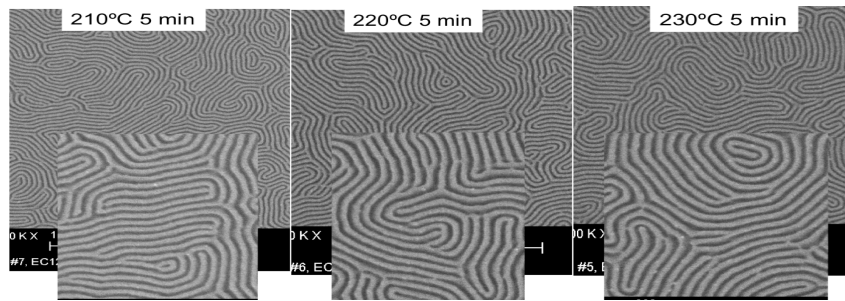

Figure 6. Good fingerprints with a range of BCP anneal temperatures from 210ºC to 230ºC.

Using the AFM, we captured scanned images for a range of bake times effective for fingerprints, from the standard 5 minutes to as short as 1 minute at 230ºC (Figure 7). In all cases, fingerprint formation was observed.
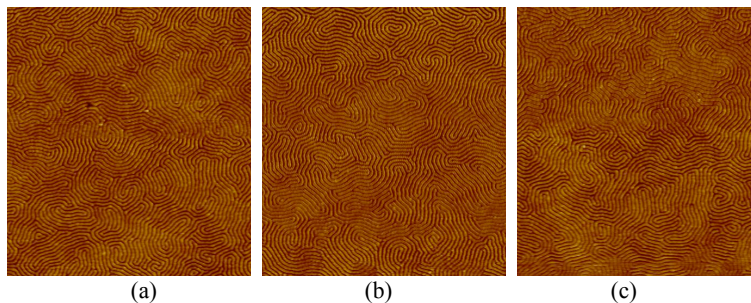

Figure 7. Good fingerprints with a range of BCP anneal times (230ºC): (a) 5 minutes, (b) 3 minutes, (c) 1 minute, viewed by AFM.

In a similar study, we also investigated BCP bake time dependence on the ability to form contact holes on the HM NL. BCP was coated and baked at 240˚C for 30–600 seconds. Figure 8 shows that contact holes can be aligned on the HM NL in as short as 30 seconds of bake time.

These results indicate wide process latitude with respect to BCP thickness, anneal temperature, and time when using the HM NL.
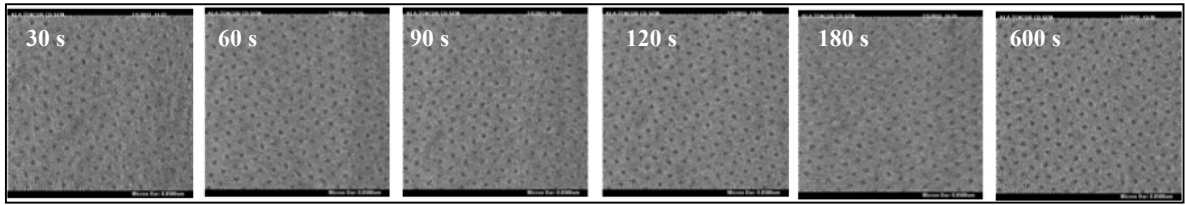

Figure 8. Contact hole formation by BCP on HM NL in 30- to 600-second bake time range.

3.3 Line/space patterning

The ability to achieve pitch multiplication on line/space pre-patterns was tested on the HM NL. Pre-patterns were prepared on the HM NL using NTD having 100-nm spaces and 600-nm pitch. After resist hard bake, the BCP was coated and annealed. CD SEM inspection (Figure 9) shows formation of lines and spaces with a pitch of approximately 26 nm.
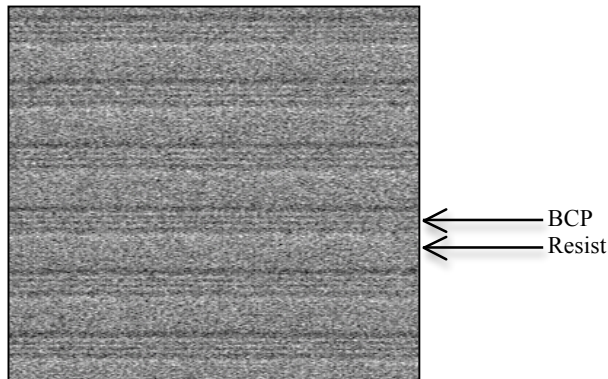

Figure 9. 3x image of dense lamellae patterns.

3.4 Contact hole patterning

Another useful aspect of DSA is the ability to pattern small contact holes to achieve contact hole critical dimension uniformity (CDU) repair or smaller CD that is possible with conventional lithography (5). Before attempting to do contact hole shrinking using BCP, we first characterized BCP contact hole formation on the HM NL.
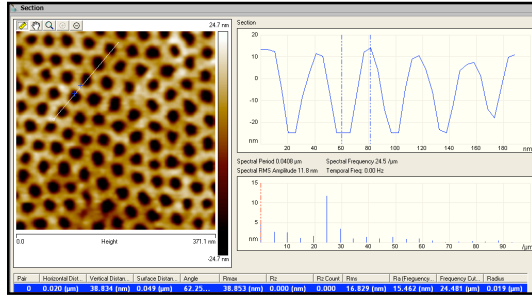

Figure 10. AFM depth analysis through contact holes formed using unpatterned wafer on HM NL.

AFM analysis of unpatterned substrates showed formation of 38-nm-deep contact holes with 20-nm pitch on the HM NL. However, we found that optimal BCP thickness for grapho-epitaxy processes is best in the 20- to 25-nm range. Contact hole shrinking was tested on patterned wafers having a target CD of 86 nm with a 130-nm pitch. The HM NL not only must have the ability to induce alignment of the BCP, it also must produce good process latitude during the pre-pattern steps. Figure 11 below shows the CD versus focus plots of the contact hole pre-patterns after litho and after the resist hard bake. A 0.21-µm DOF at 10% target CD was achieved.
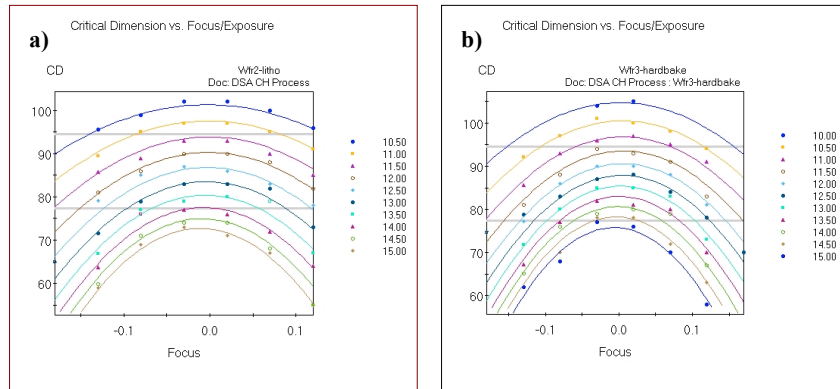

Figure 11. Bossung plots of contact hole patterns, target CD: 86 nm with 130-nm pitch, a) after litho; b) after resist hardening on HM NL.

Following pre-pattern formation, the BCP was coated and baked. The performance through focus and dose is shown in Figure 12. Good separation between the PMMA core and PS was observed through the focus and dose range.
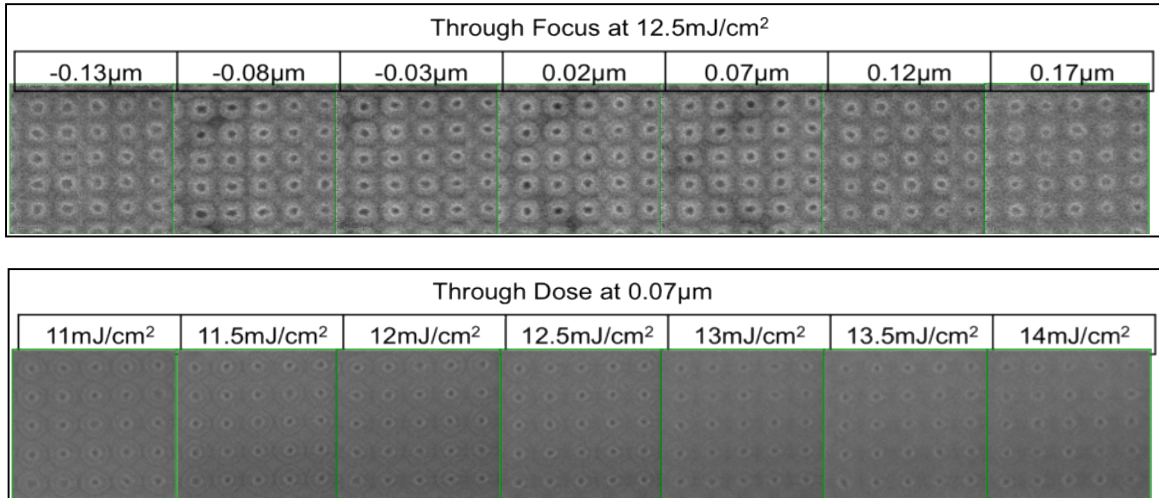
Figure 12. Performance through focus and dose of BCP on coated pre-patterns.

3.5 HM NL etch and pattern transfer

The final step in DSA patterning is pattern transfer. The PMMA core is first etched to expose the HM NL. The open pattern must then be transferred to the HM NL, the SOC, and finally the underlying substrate. In this study, etching was carried out until the SOC etch step.

PMMA removal was carried out in oxygen-rich plasma for a short time (<10 seconds), producing a contact hole opening of approximately 25 nm. Due the poor etch bias between PS and PMMA, greater than 30% of PS thickness is lost. However, the HM NL provides etch benefits. Etch selectivity between the remaining PS and the HM NL is much greater, and we were able to open 40 nm of HM NL, followed by 100 nm of SOC. The final CD was ~60 nm smaller than the initial 86-nm resist opening. Figure 13 below summarizes the overall process.
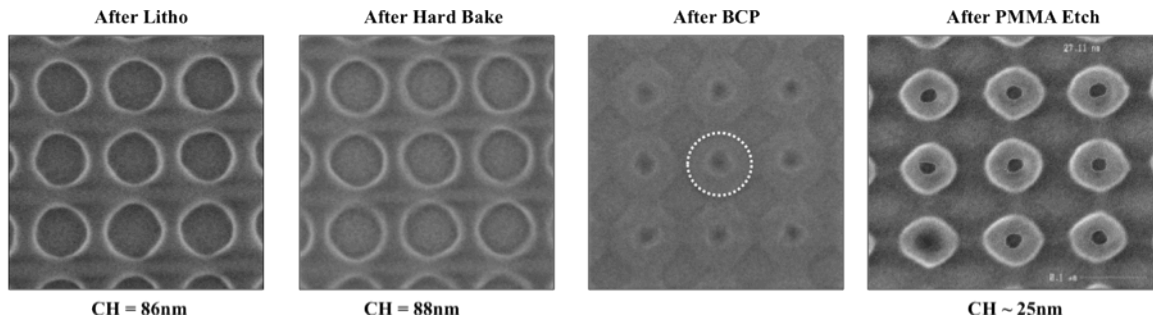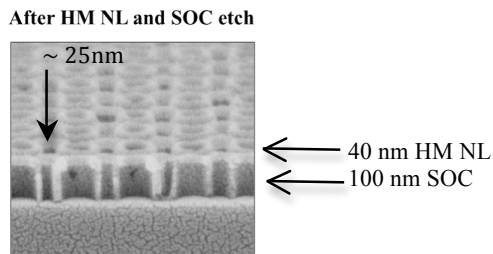

Figure 13. Contact hole (CH) shrink and pattern transfer process using HM NL and SOC layer.

4. CONCLUSIONS

We investigated an innovative solution for the DSA patterning process. The solution combines reflection control, surface energy matching, and pattern transfer capabilities into a single multifunctional material for DSA process flows using a grapho-epitaxy approach. This solution eliminates the need for three distinct layers performing similar functions. The ability of the BCP to form lines/spaces and contact holes on the HM NL was demonstrated. We also identified important factors for using BCP (thickness, bake temperature and time, surface energy) on the HM NL. Proof of concept for pattern transfer capabilities of the HM NL and SOC in a contact hole shrink process was shown. Future work will focus on exploring other novel DSA process integrations solutions.

5. ACKNOWLEDGEMENTS

6. REFERENCES

(1) Herr, D. "Direct block copolymer self-assembly for nanoelectronics fabrication," *J. Mater. Res.*, 26 (2), January 28, 2011.
(2) Cheng, J. Y.; Rettner, C. T.; Sanders, D. P.; Kim, H. C.; Hinsberg, W. D., "Dense self-assembly on sparse chemical patterns: Rectifying and multiplying lithographic patterns using block copolymers," *Advanced Materials*, 20, 3155-3158, 2008.
(3) Ruiz, R.; Kang, H. M.; Detcheverry, F. A.; Dobisz, E.; Kercher, D. S.; Albrecht, T. R.; de Pablo, J. J.; Nealey, P. F., "Density multiplication and improved lithography by directed block copolymer assembly," *Science*, 321, 936-939, 2008.
(4) Rathsack, B., Somervell, M.; Hooge, J.; Muramatsu, M.; Tanouchi, K.; Kitano, T.; Nishimura, E.; Yatsuda, K.; Nagahara, S.; Hiroyuki, I.; Akai, K.; Hayakawa, T., "Pattern scaling with directed self assembly through lithography and etch process integration," *Proc. of SPIE*, Vol. 8323, 83230B, 2012.
(5) Wuister, S. F.; Finders, J.; Peeters, E.; Van Heesch, C., "Lithography assisted self-assembly of contact holes on 300-mm wafer scale," *J. Micro/Nanolith. MEMS MOEMS*, 11(3), 031304 (July–Sept 2012).